



NRL/FR/7140--97-9823

Environmental Ocean-Bottom Backscattering Strength Based on the Mourad-Jackson Model

RALPH N. BAER
DAVID MELOY FROMM

*Acoustic Systems Branch
Acoustics Division*

February 15, 1997

REPORT DOCUMENTATION PAGE			Form Approved OMB No. 0704-0188	
Public reporting burden for this collection of information is estimated to average 1 hour per response, including the time for reviewing instructions, searching existing data sources, gathering and maintaining the data needed, and completing and reviewing the collection of information. Send comments regarding this burden estimate or any other aspect of this collection of information, including suggestions for reducing this burden, to Washington Headquarters Services, Directorate for Information Operations and Reports, 1215 Jefferson Davis Highway, Suite 1204, Arlington, VA 22202-4302, and to the Office of Management and Budget, Paperwork Reduction Project (0704-0188), Washington, DC 20503.				
1. AGENCY USE ONLY (Leave Blank)	2. REPORT DATE February 15, 1997	3. REPORT TYPE AND DATES COVERED Final, 1993 - 1996		
4. TITLE AND SUBTITLE Environmental Ocean-Bottom Backscattering Strength Upon the Mourad-Jackson Model			5. FUNDING NUMBERS PE- 61153N	
6. AUTHOR(S) Ralph N. Baer and David Meloy Fromm				
7. PERFORMING ORGANIZATION NAME(S) AND ADDRESS(ES) Naval Research Laboratory Washington, DC 20375-5320			8. PERFORMING ORGANIZATION REPORT NUMBER NRL/FR/7140--97-9823	
9. SPONSORING/MONITORING AGENCY NAME(S) AND ADDRESS(ES) Office of Naval Research 800 North Quincy Street Arlington, VA 22217-5660			10. SPONSORING/MONITORING AGENCY REPORT NUMBER	
11. SUPPLEMENTARY NOTES				
12a. DISTRIBUTION/AVAILABILITY STATEMENT Approved for public release; distribution unlimited.			12b. DISTRIBUTION CODE	
13. ABSTRACT (Maximum 200 words) Current formulations used by the Navy to model reverberation in active-acoustic-system performance scenarios are heuristic in that they do not include physical descriptors of the environment. Here we investigate a model developed originally by Pierre Mourad and Darrell Jackson of APL/UW for the backscatter component of reverberation that includes environmental descriptors in the form of eight environmental parameters, most of which can be experimentally determined in a given scenario. This model is being considered as a candidate for future incorporation in NRL's active acoustic systems performance models such as RASP, BiRASP, and BiKR. Special consideration is given to littoral (near coastal) scenarios. The water-sediment interface contribution to backscatter is, in general, benign. Although there can be more structure in the sediment volume contribution to backscatter, it is usually benign, except for when extreme values of some parameters are used. Thus, the Mourad-Jackson model can probably be incorporated into active-acoustic-system performance prediction models by fitting the parameter space and using table look-ups.				
14. SUBJECT TERMS Acoustics Ocean bottom Active system performance Reverberation Subbottom Sediment backscatter Interface Backscatter Acoustic modeling			15. NUMBER OF PAGES 16	
			16. PRICE CODE	
17. SECURITY CLASSIFICATION OF REPORT UNCLASSIFIED	18. SECURITY CLASSIFICATION OF THIS PAGE UNCLASSIFIED	19. SECURITY CLASSIFICATION OF ABSTRACT UNCLASSIFIED	20. LIMITATION OF ABSTRACT UL	

CONTENTS

INTRODUCTION	1
NUMERICAL RESULTS	3
Water-Sediment Interface Backscatter	5
Subbottom Backscatter – Typical Parameter Values	5
Subbottom Backscatter – Atypical Parameter Values	10
CONCLUSIONS AND RECOMMENDATIONS	10
ACKNOWLEDGMENTS	12
REFERENCES	12

ENVIRONMENTAL OCEAN-BOTTOM BACKSCATTERING STRENGTH BASED ON THE MOURAD-JACKSON MODEL

INTRODUCTION

Scattering in the ocean subbottom volume and scattering by the interface between the water column and the subbottom sediment region are both major contributors to acoustic reverberation in the ocean and thus significantly influence the performance of active acoustic systems. This is especially true in the shallow water that describes most of the environments present in littoral (near-coastal) regions. In these regions, it is very difficult to propagate acoustic energy without interacting with the ocean bottom.

Most acoustic reverberation and active-acoustic-system performance prediction models (see, for example Refs. 1, 2, and 3) used by the Navy, even in scientific contexts, incorporate scattering formulations that do not include physical descriptors of the ocean subbottom and bottom-ocean interface. They are often either based on ad hoc formulations such as Lambert's Law or the so-called Urlick-MacKenzie [4,5] approach. Although such formulations have been successfully used in experimental planning and modeling experimental results, they do not directly incorporate the salient environmental features that apparently influence scattering.

Pierre Mourad and Darrell Jackson of the Applied Physics Laboratory at The University of Washington (APL/UW) have developed a formulation [6] for bottom backscattering that incorporates both scattering from the water-sediment interface and scattering from the subbottom sediment volume. The environmental contribution to backscattering in the Mourad-Jackson model is contained in eight parameters. These parameters are summarized in Table 1.

The meaning of most of the Mourad and Jackson's parameters should be clear from their definitions. The loss parameter governs energy lost while propagating through the sediment volume. The volume parameter governs the amount of scattering in the sediment. The spectral strength and spectral exponent are measures of the roughness of the water-sediment interface. All parameters except water sound speed (m/s), sound-speed gradient (1/s), and spectral strength (m^4) are dimensionless.

The complete Mourad-Jackson formulation, in the form that we considered it, is described in detail in Ref. 6 and its references. Besides for these environmental parameters, the backscatter also depends on the single acoustic frequency f of the source and the incident or grazing angle θ (measured from the horizontal) of the energy interacting with the boundary.

The eight environmental parameters, although mathematically independent, are not unrelated. For example, the speed of sound in the water at the water-sediment interface appears in the sound-speed ratio v , besides for being c_0 . Also, relationships that express one parameter in terms of a perhaps more fundamental quantity and other parameters are sometimes postulated. One example of this is the following equation,

Table 1– Environmental Parameters

Symbol	Definition	Short Name
c_0	Sound speed in water at water/sediment interface (m/s)	Water sound speed
ρ	Ratio of sediment mass density to water mass density	Density ratio
ν	Ratio of sediment sound speed (at water/sediment interface) to water sound speed	Sound-speed ratio
g	Slope of sediment sound-speed profile at water/sediment interface (s^{-1})	Sound-speed gradient
δ	Ratio of imaginary wave number to real wave number for the sediment	Loss parameter
σ_2	Ratio of sediment volume scattering cross section to sediment attenuation coefficient	Volume parameter
γ	Exponent of bottom relief spectrum	Spectral exponent
w_2	Strength of bottom relief spectrum (m^4) at wave number 1 rad/m	Spectral strength

which expresses the loss parameter in terms of other parameters, and α_2 , which is the attenuation coefficient in dB/m (assuming that c_0 is in m/s) [7],

$$\delta = \frac{\alpha_2 \nu c_0 \ln 10}{40\pi f}. \quad (1)$$

The remainder of such relationships are defined and described by Mourad and Jackson. A positive value of the sound-speed gradient g indicates sound speed increases with depth in the sediment.

The long-term goal of this research is to develop an understanding of the spatial and temporal characteristics of the shallow-water monostatic and bistatic reverberation fields by investigating the dominant environmental features as a function of the acoustic frequency and the source-receiver configuration. More specifically, the objectives of this report are to study the dominant environmental parameters governing ocean bottom backscattering using the Mourad-Jackson formulation and decide on the appropriateness of the formulation as a component of an active-acoustic-system performance prediction model.

A scattering strength formulation using this model for backscattering strength is being considered as an alternative for Lambert's Law in the BiRASP [2] and BiKR [8] active-acoustic-system performance prediction models. The Mourad-Jackson formulation results in direct backscatter strength, which is a mea-

sure of the energy backscattered at the same angle θ as the incoming energy. To be useful for BiRASP or BiKR, assumptions must be made as to how the energy varies in angles other than the backscatter direction. Such assumptions are not discussed here.

The direct backscatter strength predicted by the Mourad-Jackson formulation is the sum of two terms, one representing the energy scattered by the irregular bathymetry, and the other the energy scattered by random inhomogeneities in the subbottom volume. The scattering, in turn, depends on the parameters listed in Table 1.

Originally, we attempted to analytically study how the backscattered field is influenced by each of Mourad and Jackson's parameters. We examined the water-sediment interface backscatter and the subbottom volume backscatter, both individually and together. Although a few general statements were learned, it eventually became obvious that an analytic approach would not lead to general understanding of the scattering mechanisms. This is because Mourad and Jackson had already introduced computational simplifications that would not allow at this point further analytic simplifications. Their formulation resulted in a complex combination of transcendental functions and summations that, although quite computationally feasible, does not lend itself to any analytic simplification. Thus, further work using the analytic approach was not continued and is not included here.

The most obvious fact learned by examining the equations in Mourad and Jackson's formulation is that the volume parameter σ_2 only influences the bottom volume backscatter. It does not contribute to the interface backscatter calculation.

NUMERICAL RESULTS

When an analytic approach proved to be impractical, we decided to use a numerical approach. We chose to calculate both interface scatter and bottom volume contributions to the direct backscatter strength numerically. We did this by using ranges for each parameter that span the values expected to be found in the ocean, with emphasis on littoral regions. Such parameter ranges were obtained by us both directly from cases used by Mourad and Jackson in their published work and from a substantial study [9] of parameter values by Anthony Lyons, then of Texas A & M University, using research of Hamilton [10], Hamilton and Bachman [11], and others (including Mourad and Jackson's own work).

The numerical approach proved to be more productive than the analytic approach. However, it is still not practical with existing computers and workstations to calculate the backscattering strength for all values of the 10-parameter set of values formed from combining the 8 environmental parameters with the acoustic frequency f and the incident angle θ . However, preliminary studies of variations in the backscatter function as the parameters varied over their ranges that Lyons produced showed that we could safely leave some of the parameters fixed.

We thus chose a constant value of $c_0 = 1530$ m/s. Although the backscattering strength depends on the water sound speed at the water-sediment interface, the variation is quite smooth. Also, changes in the sound speed can produce similar results to corresponding changes in the acoustic frequency, and such changes are analyzed here. Thus, major variations in backscatter strength are not omitted by taking a constant value for the parameter c_0 .

As observed, the volume parameter σ_2 does not enter into the interface backscattering calculation, and it enters into the subbottom volume backscattering calculation only as a scaling parameter. Thus, with no loss of generality in the calculations, we pick $\sigma_2 = 0.0003$ as a typical value.

Lastly, little is known from direct at-sea measurements about the spectral exponent γ . Mourad and Jackson have, in general, assumed a value of $\gamma = 3.25$ for this parameter because of this lack of experimental knowledge. We, therefore, also assumed this value for all cases reported here.

There remain five environmental parameters in addition to f and θ . We allowed the incident (grazing) angle θ to vary from 0° to 60° in steps of 2° (31 values). We used acoustic frequencies of 50, 100, 200, 400, 800, and 1600 Hz, which span the low- to mid-frequency range of interest in many past active acoustic experiments performed by NRL acousticians.

We desired to study the behavior of the backscattering strength produced by the Mourad-Jackson model mainly in the form of color or gray-scale plots with θ as the abscissa and one of the other five parameters (ρ , ν , δ , g , and w_2) as the ordinate. Therefore, we required fairly detailed sampling (similar to the sampling used for angle) for the parameter used as the ordinate and coarser sampling for the remaining parameters, which were held constant in a given plot. We thus chose parameter values as listed in Table 2.

Table 2 – Parameter Values

Parameter	Values when used as y-axis start (increment) end	Parameter values used for individual runs
ρ	1.0 (0.05) 2.5	1.00, 1.25, 1.50, 2.00, 2.50
ν	0.9 (0.01) 1.3	0.90, 0.95, 1.00, 1.10, 1.25, 1.50
δ	0.0001 (0.001) 0.0301	0.0001, 0.001, 0.01, 0.02, 0.03
g	-0.1 (-0.5) -18.1	-0.1, -0.5, -1.0, -10.0, -18.0
w_2	0.00001 (0.005) 0.18001	0.00001, 0.0001, 0.001, 0.01, 0.1

The parameter used as the ordinate is sampled by a set of 31 to 41 values, as indicated in the second column of Table 2. The three numbers in this column are respectively, the lowest value of the parameter considered, the increment in value of the parameter, and the largest value of the parameter used. The database was completed by using the set of five or six values of the remaining four parameters, as indicated in the third column. For example, we generated a set of 4,500 files to generate plots where density ratio ρ is the ordinate, corresponding to the 4,500 combinations of the six frequencies, six values of the sound-speed ratio, five values of the loss parameter, five values of the sound-speed gradient, and five values of the spectral strength. Similar sets were generated with each of the other four environmental parameters as the ordinate. There are 4,500 files for each choice of parameter for the ordinate, except for only 3,750 when the sound-speed ratio ν is the ordinate, for a total of 21,750 files.

It is possible that some combinations of parameter values are physically unobtainable. That is, no region of the ocean floor is constructed of a material that results in certain combinations of parameter values. Thus, by using the set of parameter values described in Table 2, we expect to have more than covered the region of parameter values that exist in the world's littoral regions.

Note that separate runs of the Mourad-Jackson model, as originally implemented, correspond to each grazing angle, so this database represents more than 2.3×10^7 model runs. Because of the large amount of computer time needed to generate the entire database, about a half-dozen Silicon Graphics processors were each assigned part of the task. It still took several weeks of wall clock time to produce the database.

The computational time for the 21,750 files varied by a factor of more than three orders of magnitude between slowest and fastest, depending mainly on the time needed for numerical integration of the subbottom backscatter to converge. The water-sediment interface backscattering contribution required virtually no time to calculate compared to the subbottom backscatter. If computational times for the individual runs were compared, the times would vary by even much more than three orders of magnitude.

Almost universally, higher frequency calculations took more central processor time than lower frequency calculations. Also, calculation time depended greatly on the sound-speed gradient g – the larger gradient calculations being much faster than the calculations with smaller gradients. This is an indication of deeper penetration into the sediment when the gradient is smaller. Integrations used in computing the subbottom backscatter take much longer to converge with deeper penetration.

It is impossible to illustrate this report with plots corresponding to each of the 21,750 files. Thus, only selective files are shown here. However, all of the files not contained in this report have been examined on Silicon Graphics workstation monitors.

Water-Sediment Interface Backscatter

Figure 1 is a plot showing variation of the surface component of the backscatter strength as a function of the sound-speed ratio v and grazing angle θ . The fixed parameters are the source frequency $f = 100$ Hz, the sound-speed gradient $g = 0.1 \text{ s}^{-1}$, the density ratio $\rho = 1.0$, the loss parameter $\delta = 0.0001$, and the spectral strength $w_2 = 0.1 \text{ m}^4$. The spectral strength value is quite high, although not unrealistic. The color scale as shown varies from -20 dB to -100 dB. We note a generally smooth, slow variation in the backscatter strength except for a null of at least 60 dB at $v = 1.0$. This value of the sound-speed ratio, combined with the fixed density ratio $\rho = 1.0$, essentially corresponds to there being no interface (it is acoustically “invisible”). Thus, one would expect to see minimal backscattering strength from the surface, even though it is rough. Also, as might be expected, there is no surface component to the backscatter at 0° grazing angle.

Besides for the variations of the types discussed in the previous paragraph, the surface component of the backscatter strength exhibits little structure over the ranges of values considered. Thus, further plots of this type are not shown. However, we note that the surface component, although not having much structure, can, for appropriate choices of parameter values, be much greater in value than the subbottom component of the backscatter strength. In addition, adjusting the value of the volume parameter σ_2 will change the relationship between the interface and the subbottom contributions to bottom backscatter as predicted by the Mourad-Jackson formulation because, as already stated, this parameter enters into the backscatter calculation strictly as a scaling factor.

Subbottom Backscatter – Typical Parameter Values

In the next five plots (Figs. 2-6), we investigate variations in the subbottom component of the backscatter strength. We do this by using typical, midrange values for each of the environmental parameters that is being held fixed, and allowing each parameter to be used, in turn, as the ordinate. The environmental parameters are taken as sound-speed gradient $g = 1.0 \text{ s}^{-1}$, sound-speed ratio $v = 1.1$, density ratio $\rho = 1.5$, loss parameter $\delta = 0.01$, and spectral strength $w_2 = 0.001 \text{ m}^4$. We also choose a source frequency in the middle of

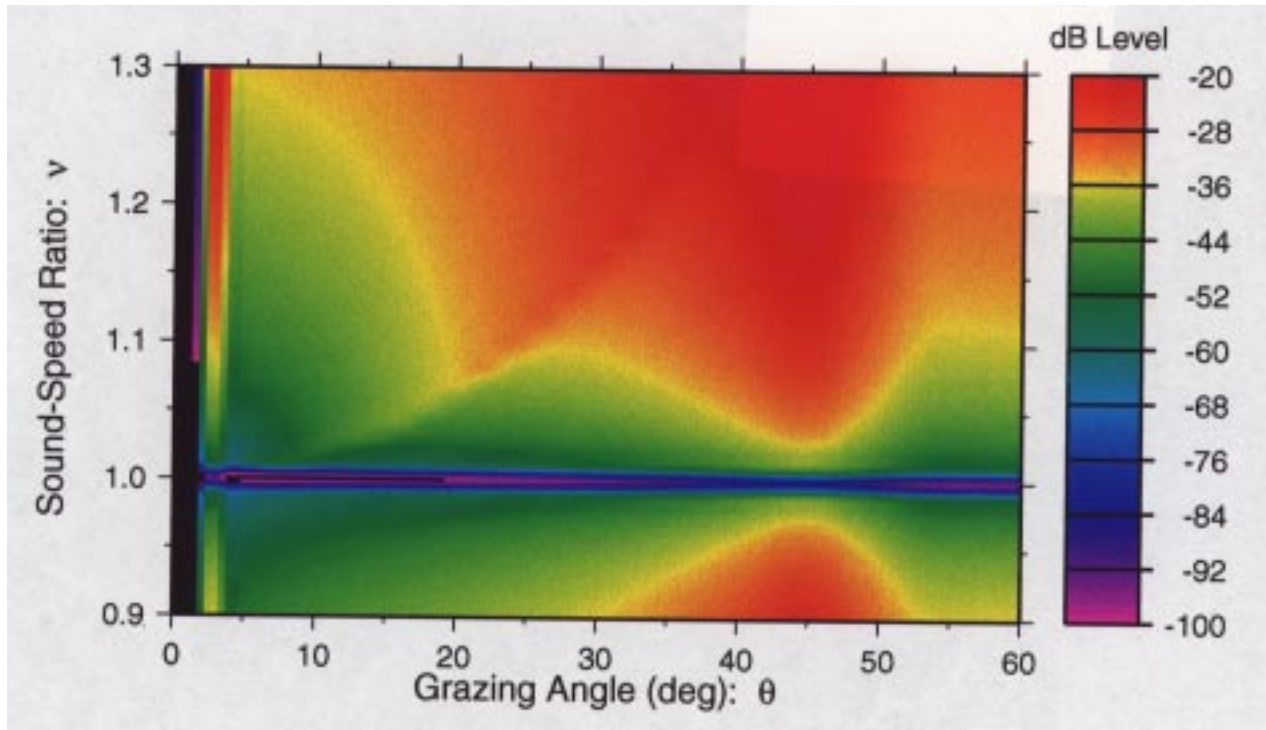


Fig. 1 – Interface backscatter strength as function of sound-speed ratio ν and grazing angle θ . Frequency $f = 100$ Hz. Environmental parameters: $g = 0.1 \text{ s}^{-1}$, $\rho = 1$, $\delta = 0.0001$, and $w_2 = 0.1 \text{ m}^4$.

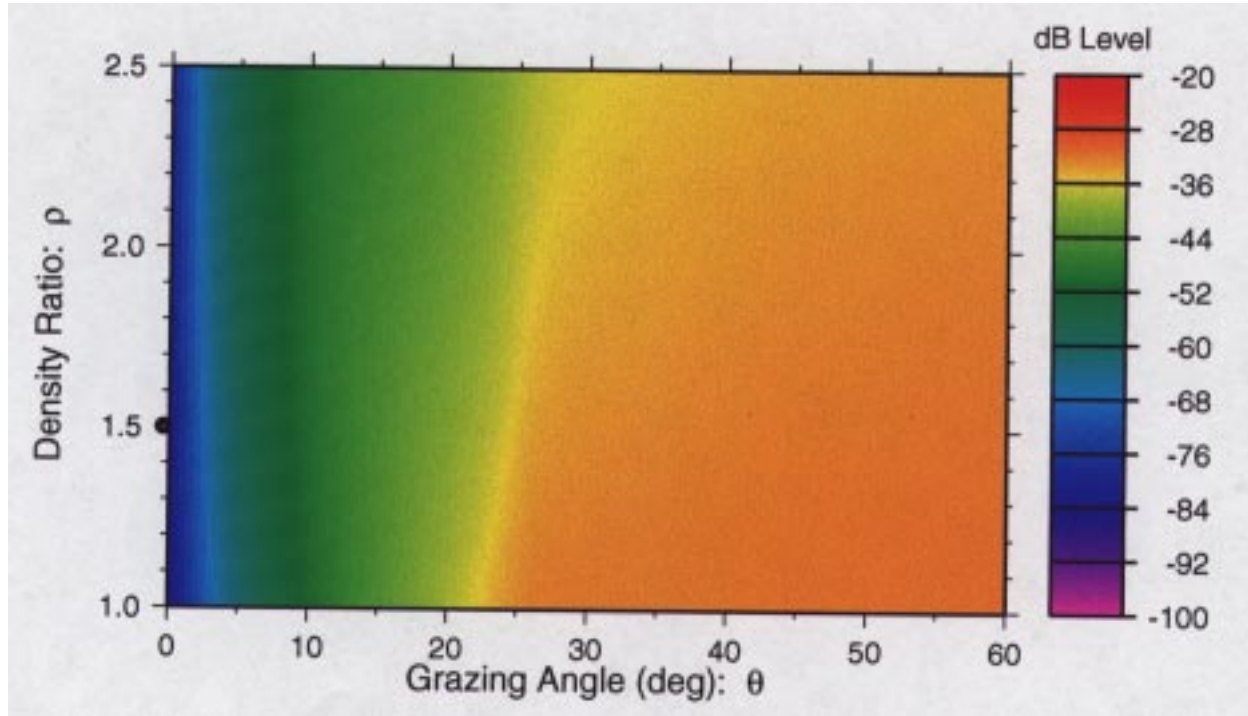


Fig. 2 – Sediment backscatter strength as function of density ratio ρ and grazing angle θ . Frequency $f = 400$ Hz. Environmental parameters: $g = 1.0 \text{ s}^{-1}$, $\nu = 1.1$, $\rho = 0.01$, and $w_2 = 0.001 \text{ m}^4$. Mark on vertical axis indicates value common to Figs. 2-6.

the range of values treated, $f = 400$ Hz. The small mark on the y-axis corresponds to the value chosen for that parameter in the remaining four plots.

First, in Fig. 2, we allow the density ratio to vary and the other parameters to be as in the previous paragraph. The subbottom backscattering strength exhibits smooth variation as a function of density ratio and grazing angles for the remainder of the “typical” parameter values. There is very little backscatter at zero degrees grazing because of lack of bottom penetration, and the backscatter increases monotonically with increasing grazing angle. At low grazing angles, the backscatter increases with increasing density ratio, while at higher grazing angle it decreases; however all of these variations are quite smooth. The smoothness of the variations indicates that the behavior could be approximated by interpolating between a relatively few, well chosen data points. Thus, the formulation appears, for this set of parameter values, to be usable as a component of an active-acoustic-system performance prediction model.

In Fig. 3, we allow the strength of the spectrum of the bottom relief (spectral strength) to vary. Note that the typical value of this parameter, used in Figs. 2 and 4-6, is near the x-axis. This is because of the great variation in magnitude of the observed values of the exponent in the bottom relief spectrum. As in the previous figure, the variations are quite smooth, indicating that the Mourad Jackson model is suitable for systems performance prediction.

In Fig. 4, we allow the sound-speed gradient in the sediment at the water-sediment interface to vary. There is somewhat more structure here than in either of the two previous plots, especially at grazing angles greater than about 30° . However, even here, the variations appear to be relatively minor, in comparison to the magnitude of the subbottom component of the backscattering strength itself, thus not precluding a simple fit to the data. Also, some of the apparent structure in the upper right of this plot is due to a slight undersampling because there are only 1147 data points (31×37). A more severe case of undersampling is illustrated in the next section of this report. This region actually contains a low-magnitude periodic variation, which would become more apparent at lower frequency.

In Fig. 5, we vary the ratio of the sediment sound speed to the water sound speed at the interface. For the range of values of ν considered, the subbottom component of the backscattering strength has a maximum value for grazing angles less than about 40° . This corresponds approximately to $\nu = 1.0$ for $\theta = 0$ and increases with increasing grazing angle. The backscattering strength increases with increasing grazing angle. Note, however, that near the point of the maximum for vertical cuts, the rate of increase with increasing grazing angles decreases.

Lastly, in Fig. 6, we allow the ratio of imaginary wave number to real wave number in the sediment (the loss parameter) to vary. As in the previous four cases, the subbottom component of the backscattering strength varies fairly smoothly. At a grazing angle of approximately 20° , the backscatter strength changes from increasing with increasing loss parameter to decreasing with increasing loss parameter. There is a null for $\delta = 0$.

In summary, Figs. 2-6 illustrate that for typical values of the environmental parameters, the subbottom component of the backscattering strength does not have any extreme variations. Therefore, the use of the Mourad-Jackson formulation as a component of an active-acoustic-system performance prediction model is not ruled out from considerations of computational efficiency. Most of the more than 20,000 situations studied look similar to the corresponding plot in Figs. 2-6, and so this same conclusion should hold in those cases also.

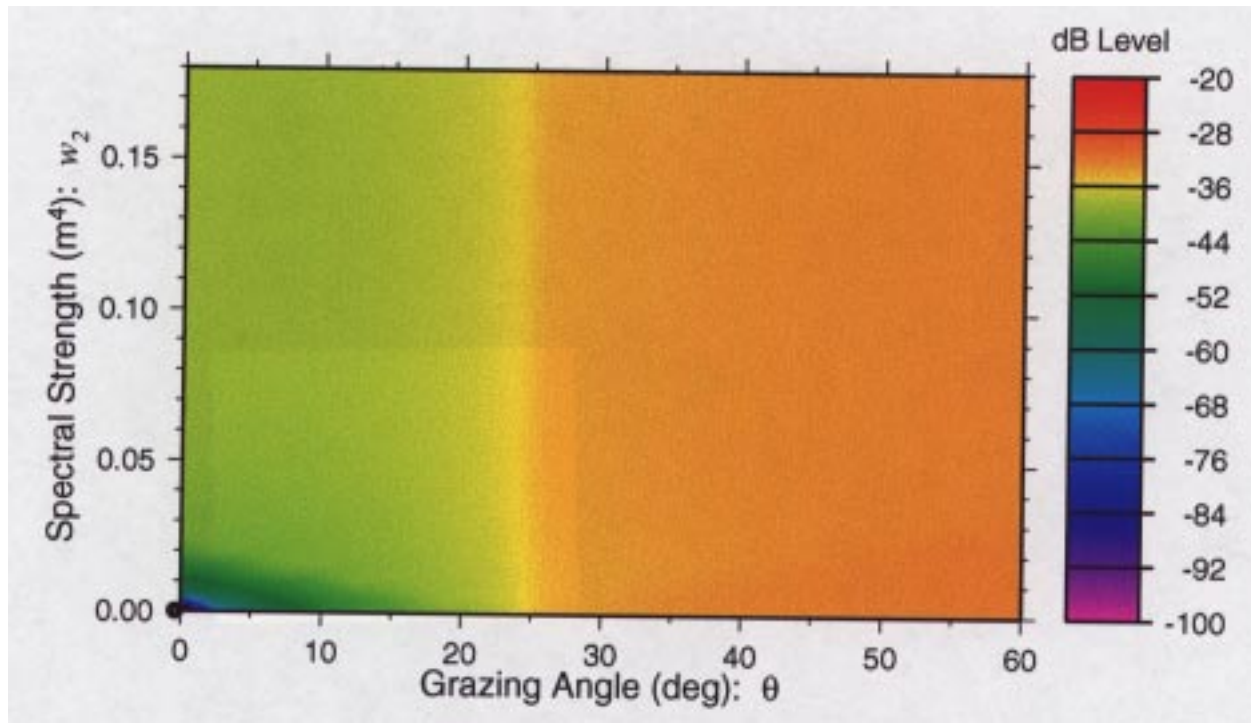


Fig. 3 – Sediment backscatter strength as function of spectral strength w_2 and grazing angle θ . Frequency $f = 400$ Hz. Environmental parameters: $g = 1.0 \text{ s}^{-1}$, $\nu = 1.1$, $\rho = 1.5$, and $\delta = 0.01$. Mark on vertical axis indicates value common to Figs. 2-6.

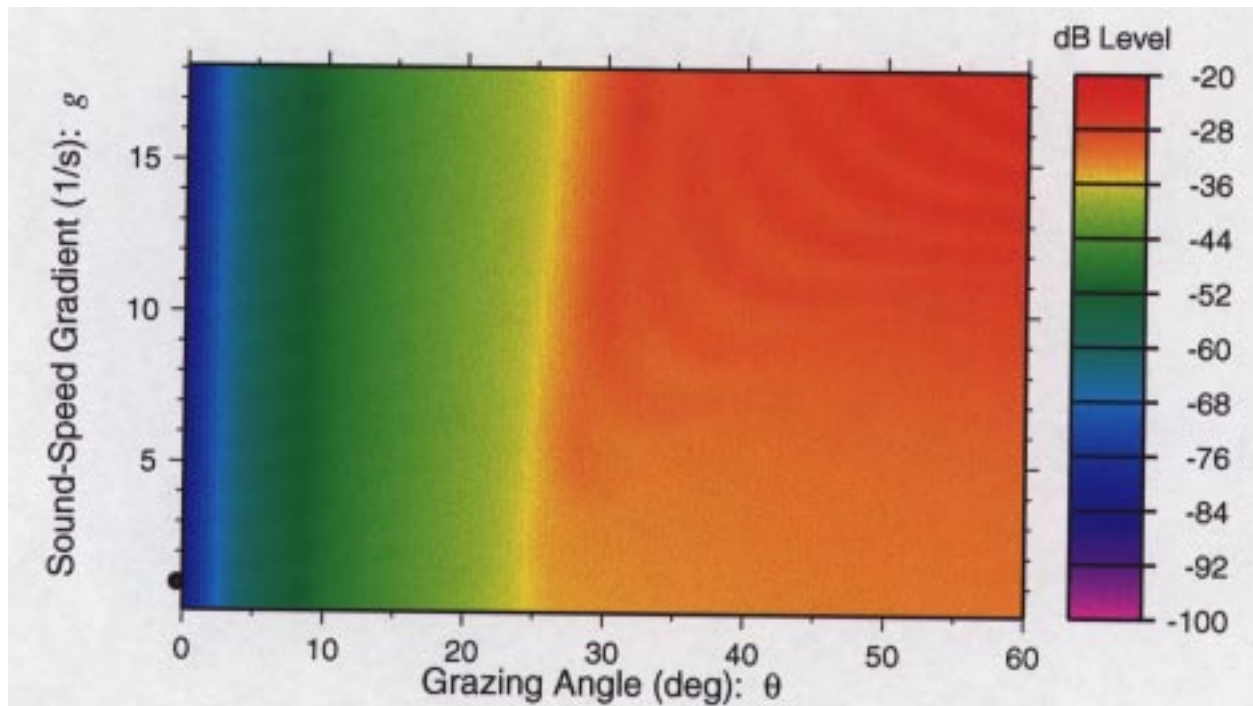


Fig. 4 – Sediment backscatter strength as function of sound-speed gradient g and grazing angle θ . Frequency $f = 400$ Hz. Environmental parameters: $\nu = 1.1$, $\rho = 1.5$, $\delta = 0.01$, and $w_2 = 0.001 \text{ m}^4$. Mark on vertical axis indicates value common to Figs. 2-6.

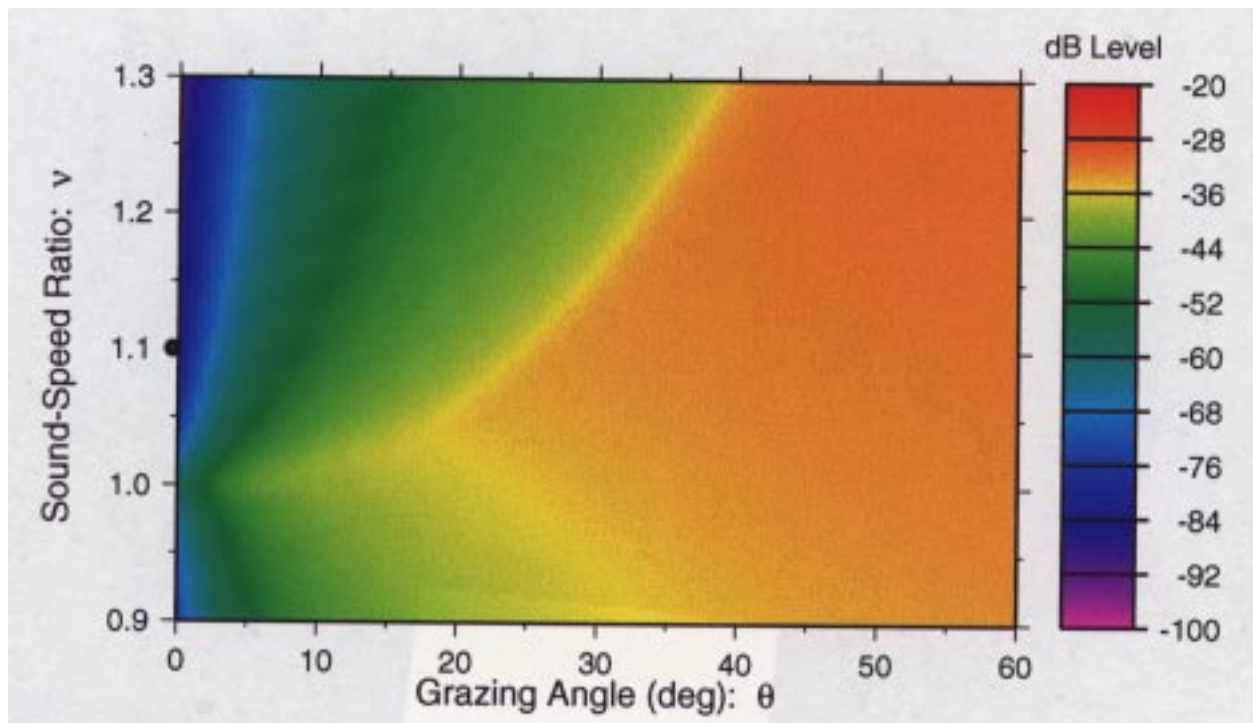


Fig. 5 – Sediment backscatter strength as function of sound-speed ratio ν and grazing angle θ . Frequency $f = 400$ Hz. Environmental parameters: $g = 1.0 \text{ s}^{-1}$, $\rho = 1.5$, $\delta = 0.01$, and $w_2 = 0.001 \text{ m}^4$. Mark on vertical axis indicates value common to Figs. 2-6.

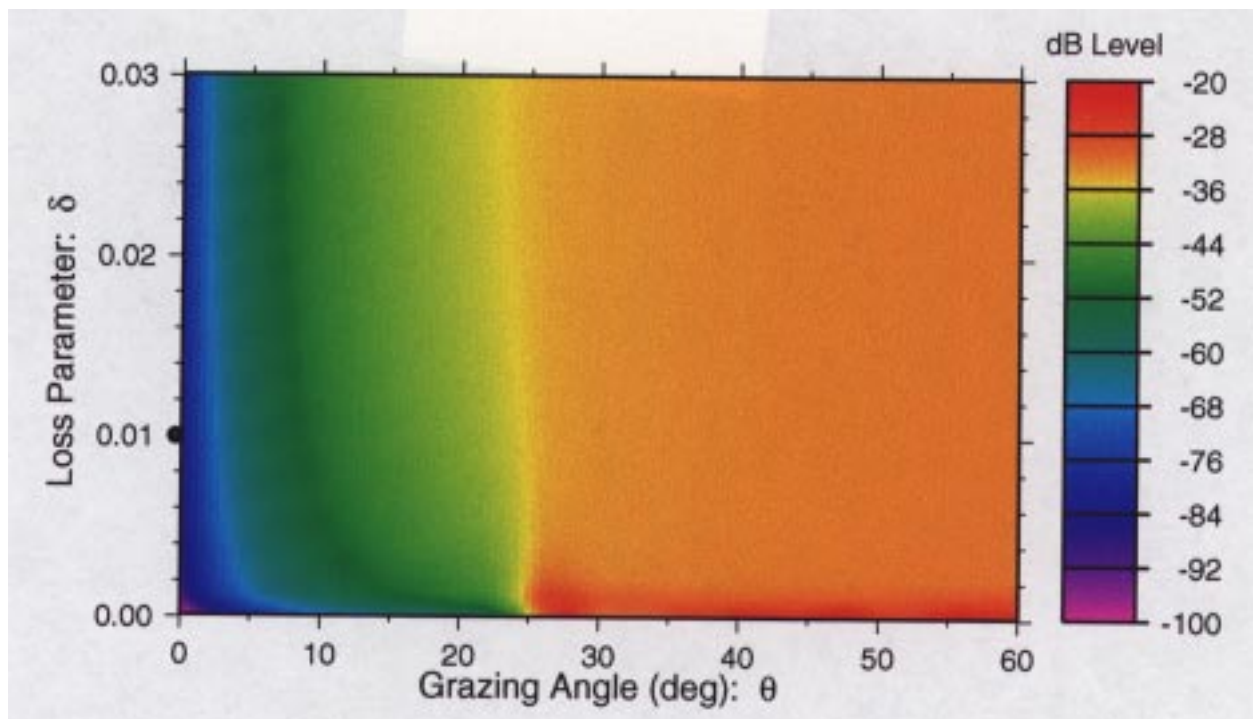


Fig. 6 – Sediment backscatter strength as function of loss parameter δ and grazing angle θ . Frequency $f = 400$ Hz. Environmental parameters: $g = 1.0 \text{ s}^{-1}$, $\nu = 1.1$, $\rho = 1.5$, and $w_2 = 0.001 \text{ m}^4$. Mark on vertical axis indicates value common to Figs. 2-6.

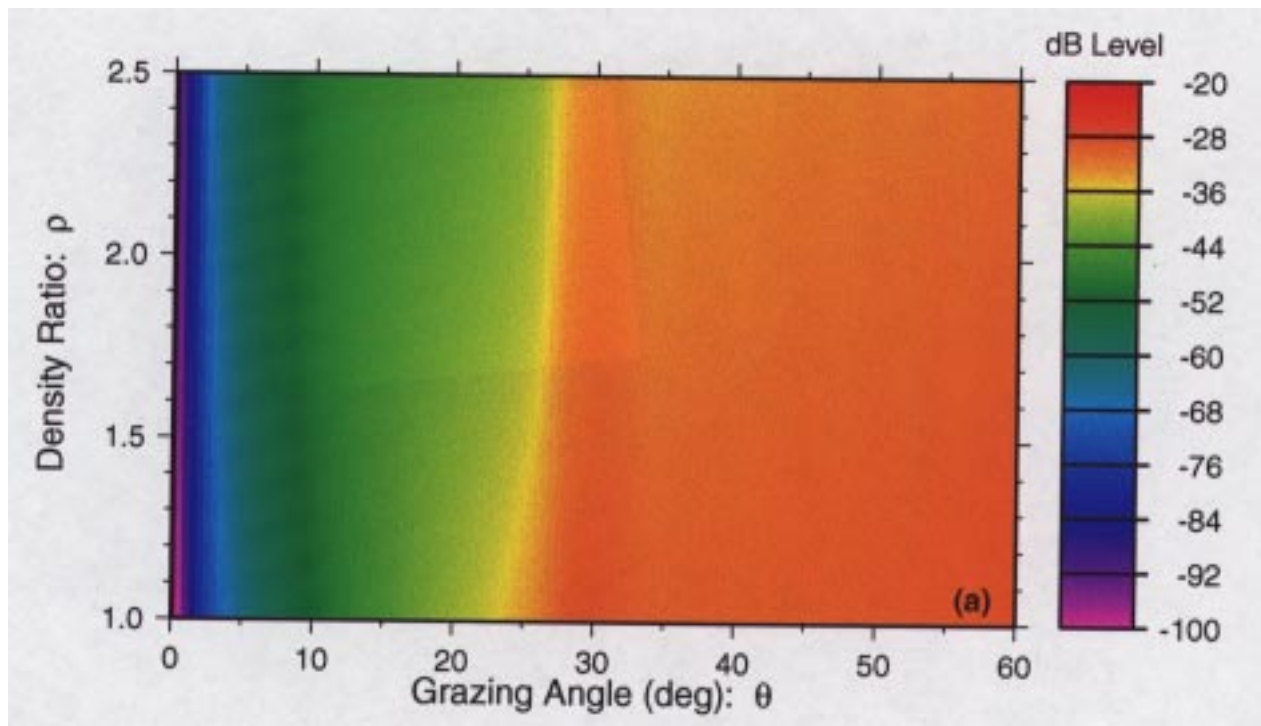
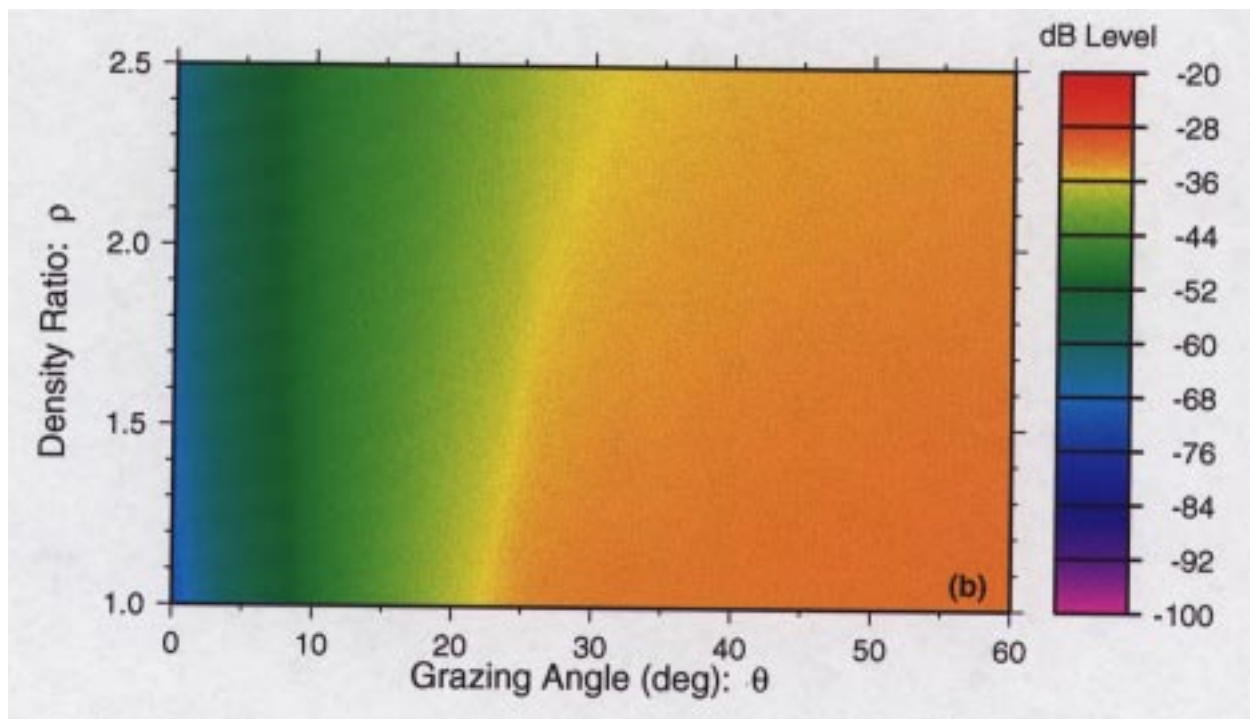
(a) $f = 50$ Hz(b) $f = 1600$ Hz

Fig. 7 – Sediment backscatter strength as function of density ratio ρ and grazing angle θ .
 Environmental parameters: $g = 1.0 \text{ s}^{-1}$, $\nu = 1.1$, $\delta = 0.01$, and $w_2 = 0.001 \text{ m}^4$.

Figures 7(a) and 7(b) are analogous to Fig. 2, with the density ratio being allowed to vary. However, in Fig. 7(a), the frequency is $f = 50$ Hz, and in Fig. 7(b), the frequency is $f = 1600$ Hz. The general level of the plots is similar to the original 400 Hz case, although, of course, the structure is not identical.

Similar plots to Figs. 3-6 at 50 Hz and 1600 Hz would also have similar levels, except in some cases structural features would be more pronounced. For example, in the 50 Hz case analogous to Fig. 4 (sound-speed gradient varying), there is a clearly periodic structure in which both grazing angle and sound-speed gradient are high. The entire structure is missing at 1600 Hz.

We now turn our attention to some situations where more structure is apparent in the subbottom component of the backscattering strength than in Figs. 2-6. In Figs. 8(a) and 8(b) (as in Fig. 3), the spectral strength is allowed to vary. The environmental parameters are the sound-speed gradient $g = 10.0 \text{ s}^{-1}$, the sound-speed ratio $v = 1.25$, the density ratio $\rho = 1.5$, and the loss parameter $\delta = 0.01$. In Fig. 8(a), the acoustic frequency is 50 Hz, and in Fig. 8(b), it is 100 Hz. The values of the density ratio and the loss parameter are as in the previous plots while the sound-speed gradient is greater by a factor of 10.

There is significantly more structure in both of these cases than in the early figures. We note a quasi-periodic pattern from the upper left to the upper right in each of the plots, with twice as many cycles at 100 Hz as at 50 Hz. In addition, certain grazing angles, which correspond to the angles where the maxima of the sinusoid-like structure intersect the $w_2 = 0$ axis, give local maxima independent of w_2 . Each of these maxima is more than 10 dB stronger than the nearby minimum.

Although the complicated structure scene of the subbottom backscatter illustrated in Figs. 8(a) and 8(b) would appear to preclude the use of a simple approximation scheme, this is probably not the case. The periodicity of the structure, the uncertainty of knowledge of environmental parameter values, and the averaging that takes place in active-acoustic-system performance calculations is expected to still allow for approximation in this and similar cases simply by smoothing the data, assuming that the structure is known and the smoothing is performed carefully.

Subbottom Backscatter – Atypical Parameter Values

In this section, we consider a case containing more extreme values in the parameter space although still within the ranges of the parameters contained in Lyons' study [9].

In Fig. 9(a), the environmental parameters chosen are the sound-speed ratio $v = 1.0$, the density ratio $\rho = 2.0$, the loss parameter $\delta = 0.0001$, and the spectral strength $w_2 = 0.0001 \text{ m}^4$. The frequency is 800 Hz. The loss parameter is very small, and thus there is little attenuation in the subbottom, allowing a lot of energy to return to the ocean volume. Much of the apparent structure in the subbottom backscatter seen in the figure is due to undersampling problems. When 100 times as many data points are plotted (ten times in each direction), Fig. 9(b) results. There is still an undersampling problem at combinations of high grazing angle and low sound-speed gradient, but the pattern is now clear. Again, even though there is visible structure, the use of properly smoothed data will not preclude usage in an active-acoustic-system performance prediction model.

CONCLUSIONS AND RECOMMENDATIONS

We have examined a great many output sets of the Mourad-Jackson scattering formulation that cover the span of values indicated by Anthony Lyons' literature search [9]. A small subset of these, consisting of

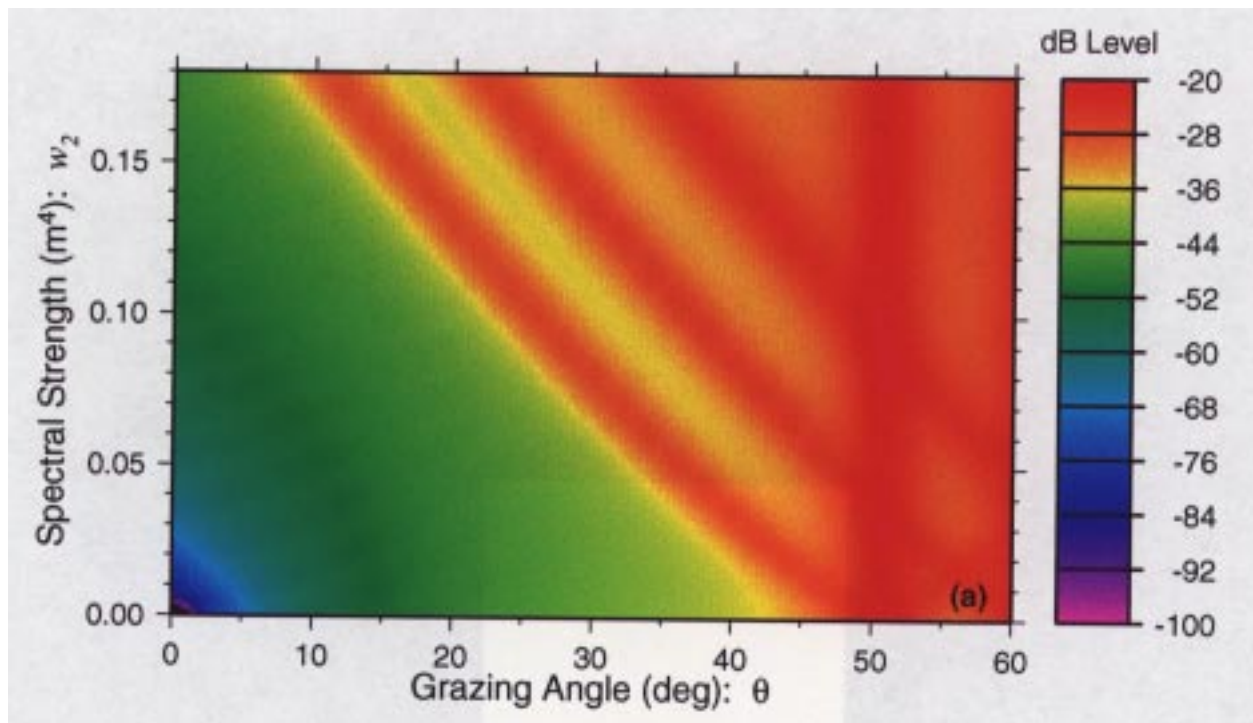
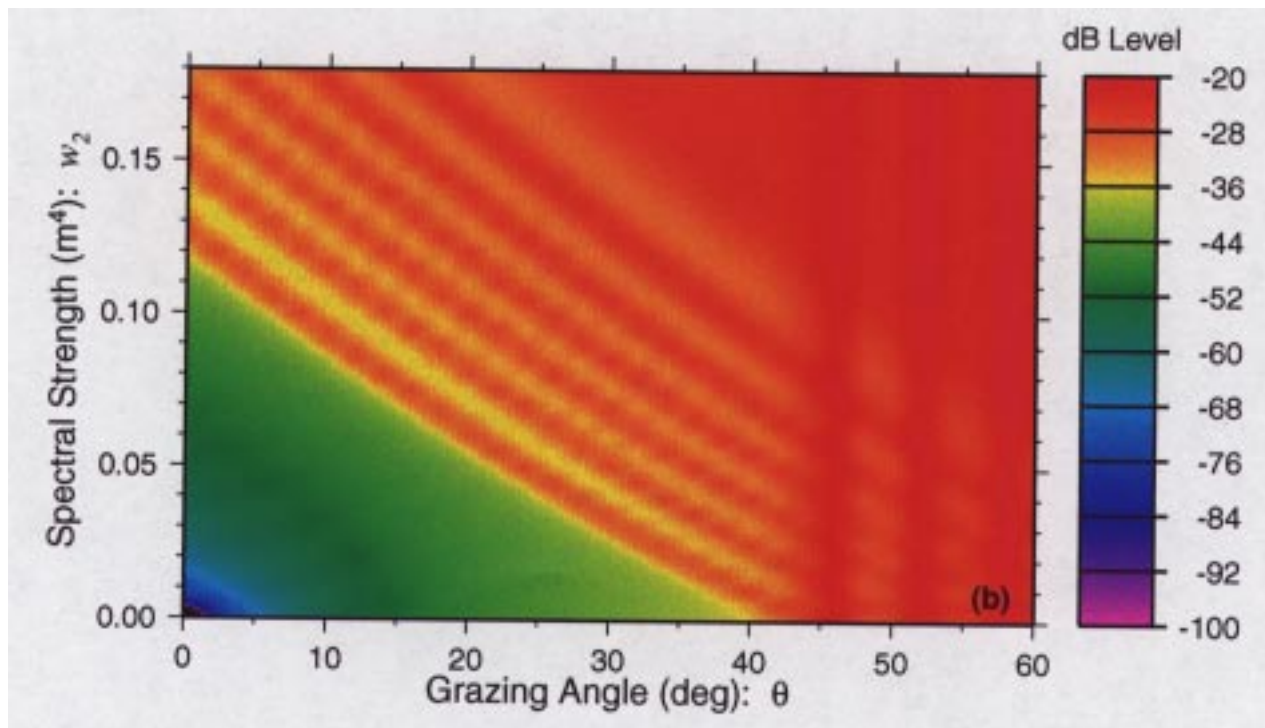
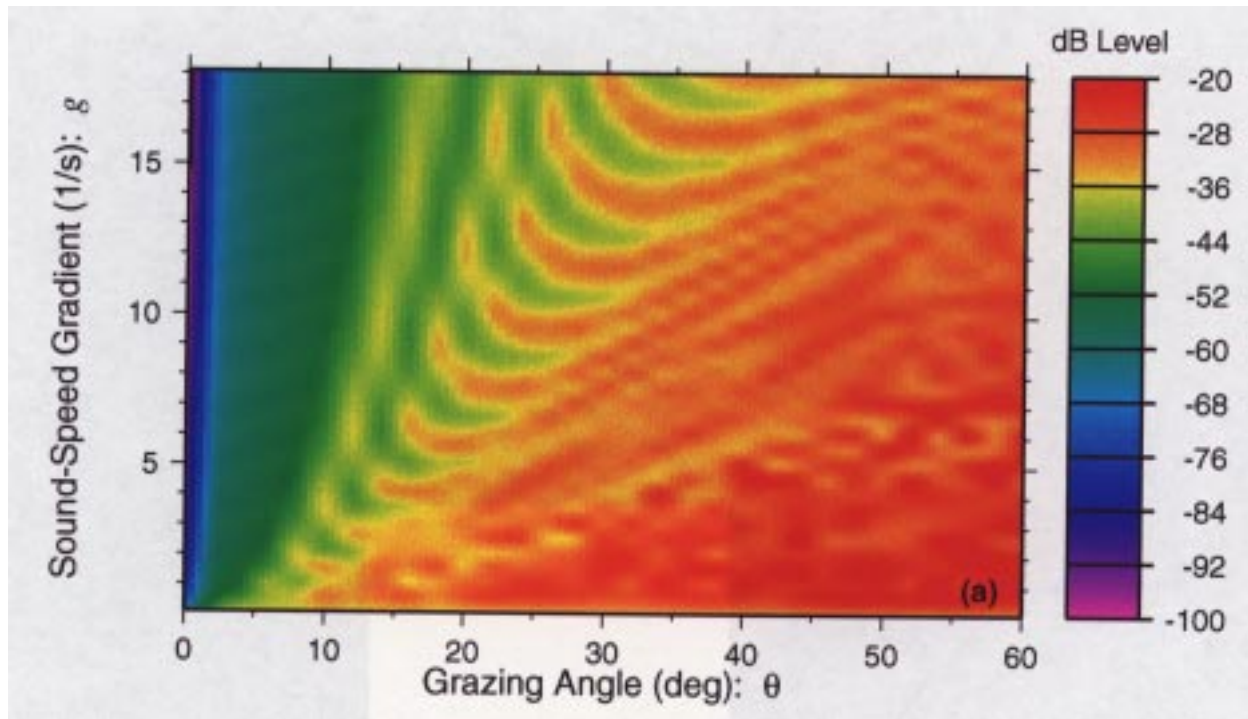
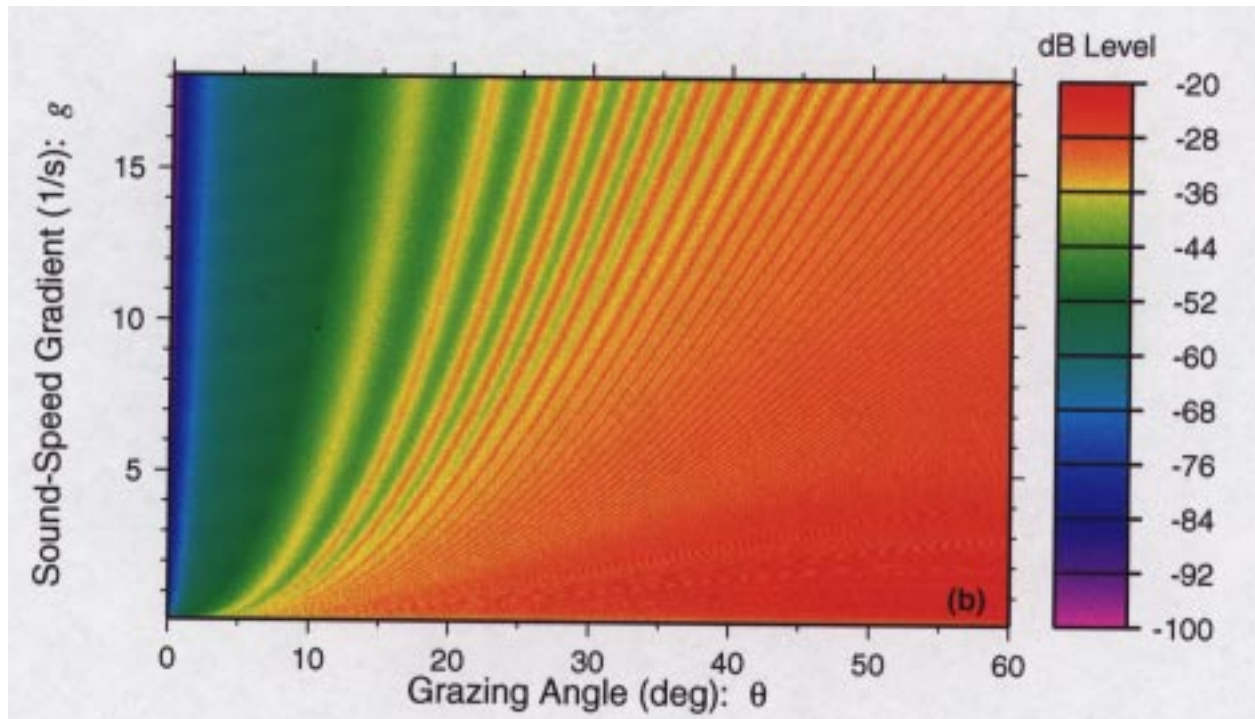
(a) $f = 50$ Hz(b) $f = 100$ Hz

Fig. 8 – Sediment backscatter strength as function of spectral strength w_2 and grazing angle θ .
Environmental parameters: $g = 10.0 \text{ s}^{-1}$, $\nu = 1.25$, $\rho = 1.5$, and $\delta = 0.01$.



(a) Standard data set



(b) Finer sampling

Fig. 9 – Sediment backscatter strength as function of sound-speed gradient g and grazing angle θ . Frequency $f = 800$ Hz. Environmental parameters: $\nu = 1.0$, $\rho = 2.0$, $\delta = 0.0001$, and $w_2 = 0.0001$ m⁴.

both typical and nontypical cases, illustrate this report. There is, in general, very little structure in the water-sediment interface contribution to the backscatter. All variations are quite benign.

There is more structure in the subbottom contribution to the backscatter when some of the environmental parameters are permitted to vary. However, for nonpathological choices of parameters, the variations appear to be such that the backscatter field can be approximated by interpolation between a relatively few well-chosen data points.

It is thus felt that the Mourad-Jackson formulation represents a viable candidate for incorporation as part of a scattering kernel in active-acoustic-system performance prediction models such as BiKR and BiRASP. It is recommended that studies be initiated in how to do this efficiently. Also, studies are needed to determine a method for efficiently extending such approximations into a general scattering kernel as opposed to the backscatter contribution discussed in this report.

ACKNOWLEDGMENTS

The authors have greatly benefited from discussions with both Dr. Pierre Mourad and Dr. Darrell Jackson of the Applied Physics Laboratory at The University of Washington (APL/UW) about many facets of the formulation of their scattering model and the code to run it. The first author also profited from discussions with Mr. Anthony Lyons of Texas A & M University about ranges and typical values for the environmental parameters in the Mourad-Jackson model. The authors thank Mr. Francis T. L. Dossey of Planning Systems, Incorporated (PSI), who performed much of the execution of the Mourad-Jackson ocean-bottom scattering model discussed in this report. In addition, he assisted in obtaining the graphical output both on computer displays and for this report. The authors also thank Mr. Joon H. Lee of NRL who assisted in the latter effort.

The research discussed in this report was supported by ONR Code 3210A.

REFERENCES

1. L. Bruce Palmer and David Meloy Fromm, "The Range-Dependent Active System Performance Model (RASP)," NRL/FR/5160-92-9383, 21 July 1992.
2. David Meloy Fromm, John P. Crockett, and L. Bruce Palmer, "BiRASP - The Bistatic Range-dependent Active System Performance Prediction Model," NRL/FR/5160-95-9723, 30 September 1996.
3. M.D. Berger, L.C. Haines, W.W. Renner, A.I. Eller, and C.E. Boucher, "Software Requirements Specification for ASPM, the Active Acoustic System Performance Model," Science Applications International Corporation Report, May 1992.
4. Robert J. Urick, *Principles of Underwater Sound, Third Edition* (McGraw-Hill, N.Y., 1983), pp. 271-280.
5. K.V. MacKenzie, "Bottom Reverberation for 530 and 1030-cps Sound in Deep Water," *J. Acoust. Soc. Am.* **33**, 1498-1504 (1961).
6. Pierre D. Mourad and Darrell R. Jackson, "A Model/Data Comparison for Low-Frequency Bottom Backscatter," *J. Acoust. Soc. Am.* **94**, 344-358 (1993).

7. Pierre D. Mourad and Darrell R. Jackson, "High Frequency Sonar Equation Models for Bottom Backscatter and Forward Loss," in *Proceedings of Oceans '89* (Marine Technology Society and IEEE), pp. 1168-1175 (1989).
8. David Meloy Fromm and Kenneth H. Luther, "BiKR – A Range-dependent, Normal-Mode Performance Prediction Model for Bistatic Geometries," NRL/FR/7140–95-9786, in preparation.
9. Anthony P. Lyons, Texas Agriculture and Mining University (now at SACLANTCEN Undersea Research Center, La Spezia, Italy), personal communication, 1993.
10. E.L. Hamilton, "Geoacoustic Modeling of the Sea Floor," *J. Acoust. Soc. Am.* **68**, 1313-1340 (1980) and earlier references mentioned therein.
11. E.L. Hamilton and R.T. Bachman, "Sound Velocity and Related Properties of Marine Sediments," *J. Acoust. Soc. Am.* **72**, 1891-1904 (1982).